Very Small Ultra-Wide-Band MMIC Magic T and Applications to Combiners and Dividers

TSUNEO TOKUMITSU, MEMBER, IEEE, SHINJI HARA, MEMBER, IEEE, AND MASAYOSHI AIKAWA, MEMBER, IEEE

Abstract—**An FET-sized 1–18 GHz monolithic active magic T (180° hybrid) is proposed. It unifies two different dividers, electrically isolated from each other, in a novel GaAs FET electrode configuration, viz. the LUFET concept. Its characteristics and experiment results are presented. Applications of the magic T to miniature wide-band RF signal processing modules such as dividers, combiners, and switches are described.**

I. Introduction

COMBINERS, dividers, and magic T's are fundamental and important circuit functions used for microwave and millimeter-wave circuits. However, these functions, which are traditionally constructed with quarter-wavelength transmission lines, occupy large areas in MMIC chips, and the bandwidths are limited due to the electrical line lengths [1], [2]. The functions should be miniaturized for applications to RF signal processing. Recently, traveling wave active combiners and dividers which employ GaAs FET's for compact size and wide-band operation were reported [3]–[5]. However, the circuit configuration is still large as well as extremely complicated because several GaAs FET's and many spiral inductors are packed on a chip.

In this paper, a very simple monolithic active magic T composed of a GaAs FET with two gate fingers and coplanar lines is proposed. The most significant innovation of the magic T is a novel circuit structure which effectively uses the two-gate GaAs FET configuration to unify two different dividers within the electrode configuration. This magic T is based on the line unified FET (LUFET) concept, which was previously proposed by the authors for FET-sized, wide-band circuit function modules [6]. An advantage of the proposed magic T is that it significantly reduces MMIC chip size, as well as operates over an ultrawide-band, due to the minimum use of GaAs FET's and the absence of spiral inductors. Divider/combiner modules in simple configurations are also designed with the active magic T. Such a miniature wide-band magic T allows applications to various MMIC's for RF signal processing, such as mixers, vector combiners, and switch matrixes.

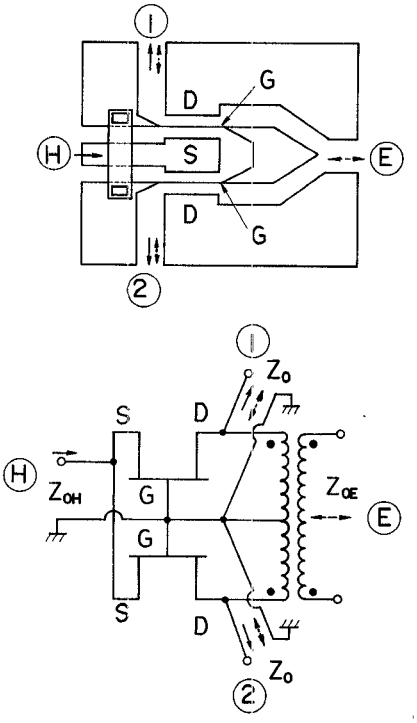

Fig. 1. Configuration and equivalent circuit diagram of the magic T LUFET.

II. Magic T Configuration and Design

The schematic and equivalent circuit of the proposed magic T are shown in Fig. 1, where Z_{0H}, Z_{0E}, and Z_0 are the transmission line impedances of ports Ⓗ, Ⓔ, and ① and ②, respectively. This active magic T is composed of a two-gate GaAs FET and coplanar transmission lines unified within the electrode locations of drain–gate–source–gate–drain. An in-phase power divider, with coplanar waveguide input port Ⓗ and slotline output ports ① and ② electrically isolated from one another, is realized by the electrode placement, where the gates serve as the

Manuscript received March 31, 1989; revised July 21, 1989.

T. Tokumitsu and S. Hara are with ATR Optical and Radio Communications Research Laboratories, Inuidani, Seika-cho, Soraku-gun, Kyoto 619-01, Japan.

M. Aikawa was with ATR Optical and Radio Communications Research Laboratories, Kyoto, Japan. He is now with NTT Radio Communication Systems Laboratories, Yokosuka 238-03, Japan.

IEEE Log Number 8930947.

module's common electrode. Furthermore, a slotline series T junction as an out-of-phase power divider, with slotline input port Ⓔ and slotline output ports ① and ②, is formed with a conductive pad connecting the two gate electrodes and two drain electrodes, one on each side of the pad. In other words, two different dividers are unified in the GaAs FET electrode allocation, while the two dividers are isolated from each other because of the orthogonal mode effect and the unilateral effect of the GaAs FET. The impedance match at port Ⓗ is determined by the transconductance of the two-gate GaAs FET. The impedance at the other ports and the isolation characteristics between ports ① and ② are determined by the slotline T junction and the equivalent resistance, R_{DG}, observed or connected between the drain and the gate of each GaAs FET.

This magic T LUFET operates over an ultra-wide-band frequency range because the parasitics in the GaAs FET's are terminated with low impedance Z_0 and because of the absence of frequency-dependent circuitry such as quarter-wavelength transmission lines and spiral inductors. Orthogonal mode analysis based on the symmetrical configuration of the magic T yields the following equations characterizing the magic T [7], where the FET is assumed to be a combination of the transconductance g_m and negligible gate–source capacitance C_{gs} only:

$$S_{ⒽⒽ} = \frac{1-2g_mZ_{0H}}{1+2g_mZ_{0H}} \tag{1}$$

$$|S_{①Ⓗ}| = |S_{②Ⓗ}| = \frac{2g_m\sqrt{Z_{0H}Z_0}}{1+2g_mZ_{0H}} \cdot \frac{R_{DG}}{R_{DG}+Z_0} \tag{2}$$

$$|S_{①①}| = |S_{②②}| = \frac{|\Gamma_{+-}+\Gamma_{++}|}{2} \tag{3}$$

$$|S_{①②}| = |S_{②①}| = \frac{|\Gamma_{+-}-\Gamma_{++}|}{2} \tag{4}$$

$$|S_{ⒺⒺ}| = |\Gamma_{+-}| \tag{5}$$

$$|S_{①Ⓔ}| = |S_{②Ⓔ}| = |S_{Ⓔ①}| = |S_{Ⓔ②}| = \sqrt{\frac{1-|\Gamma_{+-}|^2}{2}} \cdot \frac{2R_{DG}}{2R_{DG}+Z_0} \tag{6}$$

where the reflection coefficients Γ_{+-} and Γ_{++} at port ① in each excitation mode are given by the following equations:

$$\text{Odd: } \Gamma_{+-} = \frac{(Z_{0E}\|2R_{DG})-2Z_0}{(Z_{0E}\|2R_{DG})+2Z_0}$$

$$\text{Even: } \Gamma_{++} = \frac{R_{DG}-Z_0}{R_{DG}+Z_0}.$$

The isolation from ports ① and ② to port Ⓗ and the isolation between ports Ⓗ and Ⓔ are due to the unilateral characteristic of each GaAs FET and the orthogonal mode effect in the magic T's configuration, respectively.

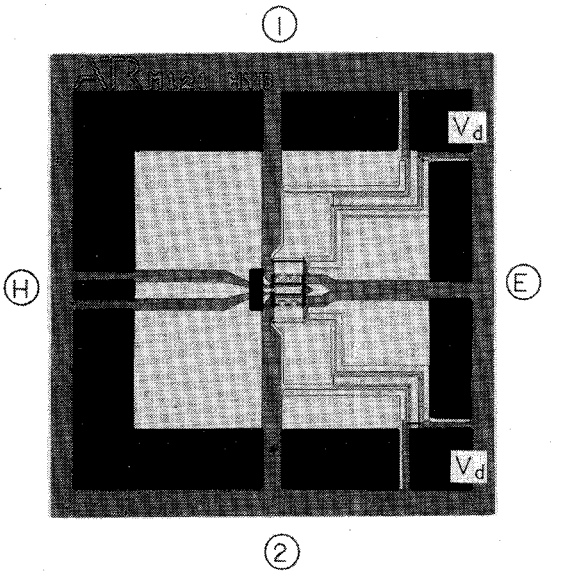

Fig. 2. Photograph of the magic T LUFET on a 1 mm × 1 mm chip (intrinsic area is only 0.15 mm × 0.25 mm).

The reflection coefficient $|S_{ⒽⒽ}|$ is at its minimum, that is, zero, when $2g_mZ_0 = 1$, while the power coupling $|S_{①Ⓗ}|$, $|S_{②Ⓗ}|$ is −6 dB. The power coupling $|S_{①Ⓗ}|$, $|S_{②Ⓔ}|$ is less than −3.5 dB. The difference between the couplings can be less than 2 dB when $2g_mZ_0$ is greater than 1.2. The resistor R_{DG} acts to reduce the reflection coefficient at ports ① and ② and to increase the isolation between ports ① and ②.

III. Experimental Results

A photograph and the performance of the fabricated magic T are shown in Fig. 2 and Fig. 3, respectively. The chip size is 1 mm × 1 mm × 0.6 mm, while the intrinsic area is only 150 μm × 250 μm. This active magic T has been fabricated using epitaxial growth 0.5-μm-gate-length GaAs FET's with a cutoff frequency of approximately 20 GHz. The unit gate width is 75 μm.

The ultra-wide-band characteristics of the magic T have been confirmed through on-wafer measurements up to 18 GHz, as shown in Fig. 3. Drain bias V_d (3 V) for each drain electrode is supplied through the pads and MIM capacitors. Source bias, through a wide-band bias T and an on-wafer-measurement probe attached at port Ⓗ, is adjusted for a transconductance better than 20 mS. The typical current drawn is 10 mA and power consumption is only 30 mW, where I_{dss} of the 150-μm-gate-width GaAs FET is between 30 and 50 mA. The measured performance (solid lines) is as follows: coupling loss from port Ⓗ or Ⓔ to ports ① and ② is within 5 dB ± 1 dB; return loss at each port is greater than 10 dB; and isolation is greater than 20 dB except between ports ① and ②, where it is about 10 dB. The dashed lines in Fig. 3 show the calculated performance of the active magic T. The calculation is performed with a typical small-signal equivalent circuit of the GaAs FET and an R_{DG} value (700 Ω) for both

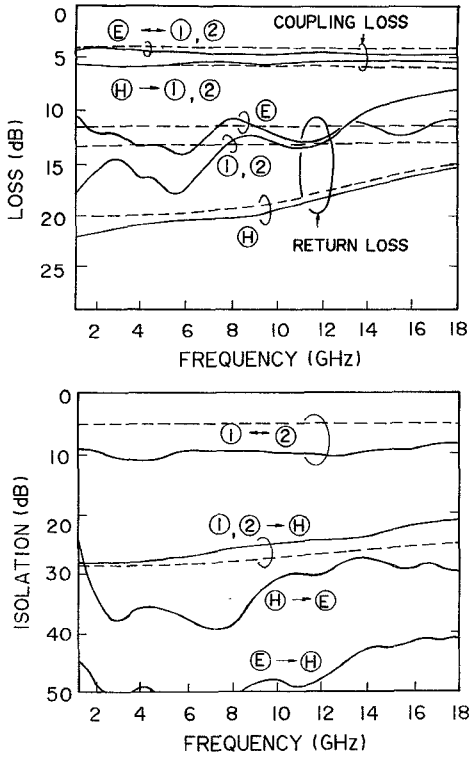

Fig. 3. Performance of the magic T LUFET (solid line: measured; dashed line: predicted).

excitation modes. That the measured isolation between ports ① and ② is better than predicted is believed to be due to the module's configuration. A spatial coupling, for example, between the coplanar waveguide and the slotlines separated by the gate electrodes improves Γ_{++}, thus improving the isolation. The spatial coupling occurs in only the even-mode excitation and reduces the equivalent resistance R_{DG} for this mode. Isolation between ports ① and ② is improved by 2 dB when isolation from ports ① and ② to port Ⓗ is about 25 dB, as shown in Fig. 3. Thus, the equivalent resistance R_{DG} in each excitation mode should be estimated individually for more accurate design.

The magic T LUFET can be applied to miniaturized wide-band balanced mixers. Fig. 4 shows the output power versus input power characteristics of the magic T, where two power-incident ports Ⓗ and Ⓔ are examined. The characteristic from port Ⓔ to port ① exhibits good linearity for input powers up to 18 dBm and more, while that from port Ⓗ to port ① begins a gain compression near 5 dBm. Thus, LO power from port Ⓔ can be sufficiently high to achieve low conversion loss.

Additionally, the magic T LUFET can be changed to another LUFET merely by interchanging the supplied voltages, due to the change in electrode locations from drain–gate–source–gate–drain to source–gate–drain–gate–source. This LUFET operates as a mode splitter, where in-phase signals and out-of-phase signals from ports ① and ② emerge at port Ⓗ and at port Ⓔ respectively, with an insertion loss of about 3 dB for each. In the next section, attention will be given to a signal

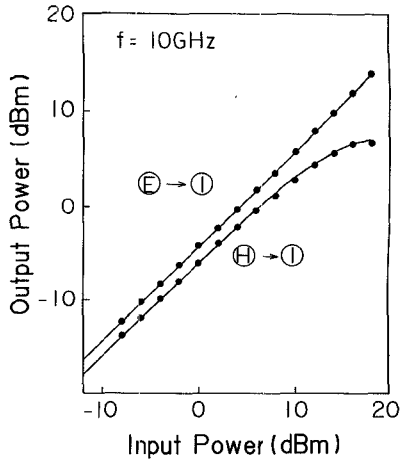

Fig. 4. Output power versus input power characteristics of the magic T LUFET.

divider/combiner that employs this LUFET, called a mode-splitter LUFET, combined with the magic T LUFET.

IV. Signal Divider/Combiners

A photograph and the equivalent circuit diagram of a signal divider/combiner utilizing the magic T LUFET are shown in Fig. 5. The chip size is 1 mm×1 mm×0.6 mm. Two magic T's are combined symmetrically at ports ① and ② and port Ⓔ, where a shunt resistor R_0 is connected. The characteristics of signal divider/combiner 1 and the magic T are represented in similar fashion because the only changes in the above equations are R_{DG} to $R_{DG}/2$ and Z_{0E} to R_0. Therefore, signal power division from port (H_1) or (H_2) to ports ① and ② is achieved maintaining port isolation in the magic T. Isolation between output ports ① and ② is significantly improved by increasing the R_0 value. Fig. 6 shows the performance of fabricated divider/combiner 1 shown in Fig. 5, where R_0 is given two different values, 50 Ω and infinity. Coupling loss from port (H_1) or (H_2) to ports ① and ② is between 5 and 6 dB, and almost the same for both R_0 values, while isolation between ports ① and ② is changed considerably by the R_0 value because resistor R_0 is connected in series between ports ① and ②. Return loss at ports (H_1) and (H_2) is better than 13 dB for both R_0 values, up to 18 GHz.

Advantages of divider/combiner 1 are that it operates in an ultra-wideband frequency range, and offers the following useful functions in a small MMIC chip size. This module divides RF incident signals, $\dot{A}$ and $\dot{B}$ on ports (H_1) and (H_2), respectively and simultaneously generates the same combined signals, $(\dot{A}+\dot{B})/2$, at ports ① and ② with good isolation. This module can also be used to change the signal path with (H_1)–(H_2) isolation better than 20 dB, as shown in Fig. 7, by controlling the gate–source voltages for the two GaAs FET's. In Fig. 7,

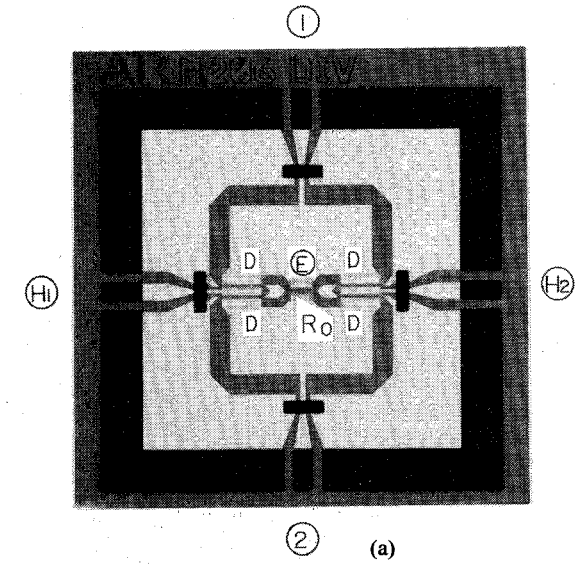

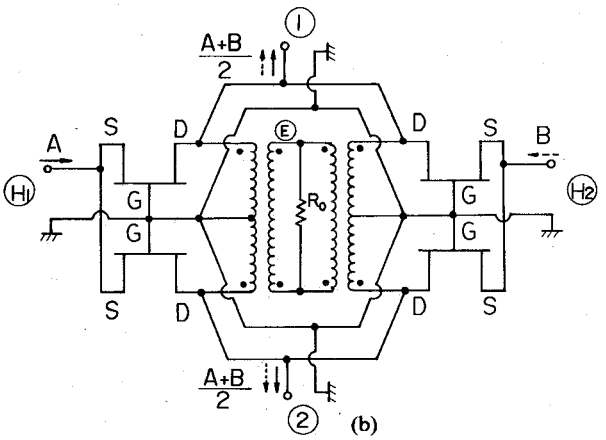

Fig. 5. Configuration and equivalent circuit diagram of signal divider/combiner 1 designed with the magic T LUFET. (a) Photograph. (b) Equivalent circuit diagram.

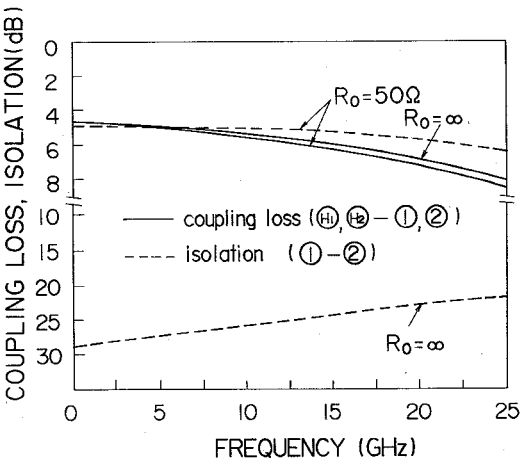

Fig. 6. Performance of fabricated divider/combiner 1.

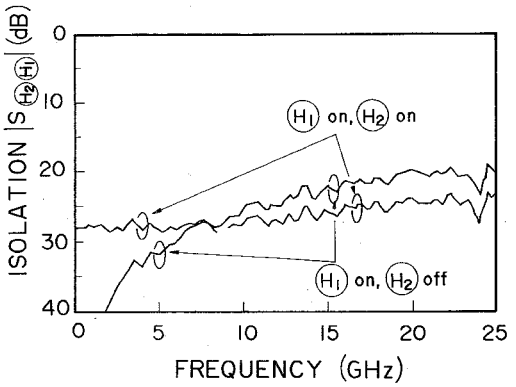

Fig. 7. Measured isolation between ports (H_1) and (H_2) for divider/combiner 1.

the two-gate GaAs FET on port (H_1) is in the on-state and that on port (H_2) is switched. It can also switch the signal flow between ports ① and ② by controlling the value of R_0. These functions are not possible with passive circuits.

Fig. 8 shows another signal divider/combiner. This module, which consists of a magic T LUFET and a mode splitter LUFET, has almost the same configuration as signal divider/combiner 1, the exception being the electrode locations of source–gate–drain–gate–source in the right two-gate GaAs FET. The chip size is 1 mm×1 mm. This module, divider/combiner 2, divides an incident signal $\dot{A}$ from port (H_1) to ports ①, ②, and (H_2), and delivers incident signals $\dot{B}$ and $\dot{C}$ from ports ① and ②, respectively, only to port (H_2) because of the unilateral characteristic of each two-gate GaAs FET and isolation between ports ① and ②. Incident and delivered signal voltages are shown in Fig. 8. Fig. 9 shows coupling loss–frequency characteristics of divider/combiner 2. In the

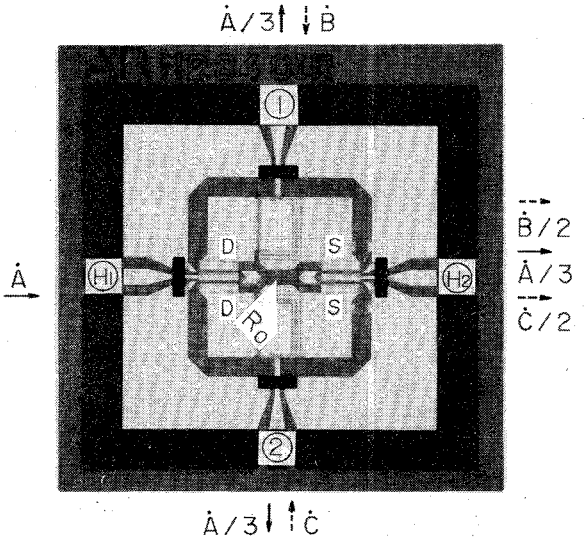

Fig. 8. Configuration of signal divider/combiner 2 designed with the magic T and mode splitter LUFET's.

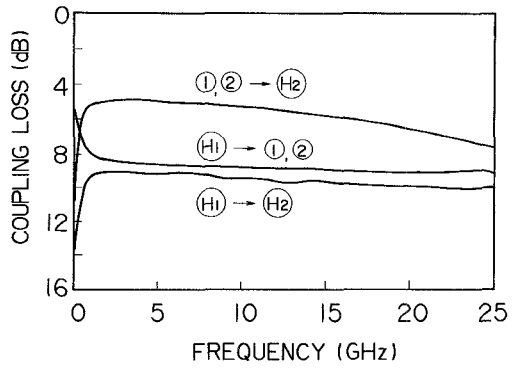

Fig. 9. Coupling loss characteristics of signal divider/combiner 2.

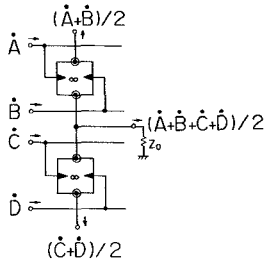

Fig. 10. Four-port signal combiner using two divider/combiner modules.

region from 1 to 18 GHz, coupling loss from port (H_1) to ports ①, ②, and (H_2), and that from port ① or ② to port (H_2) are 9 dB±1 dB and 6 dB±1 dB respectively. Return loss at ports ①, ②, and (H_1) is better than 10 dB. Isolation from port ① or ② to port (H_1) and between ports ① and ② is better than 25 dB and 15 dB, respectively, when R_0 is 200 Ω. This module is also a functional module, which is not possible with passive circuits.

These modules, as well as the magic T, are so small that higher level signal processing circuits can be designed with little concern for chip size. In the next section, some applications of signal divider/combiner 1 are referred to by symbol.

V. Signal Divider/Combiner Applications

Fig. 10 shows a combination of two divider/combiner modules, i.e., a four-port signal combiner. The square represents the divider/combiner module in Fig. 5; the triangle, which suggests directivity, represents the two-gate GaAs FET; and the dot inside a circle represents the slotline–CPW T junction. This circuit combines four input signals, $\dot{A}$, $\dot{B}$, $\dot{C}$, and $\dot{D}$, when all FET's are in the on-state, indicated by black triangles in the illustration. In addition to this output, i.e., $(\dot{A}+\dot{B}+\dot{C}+\dot{D})/2$, other outputs, such as $(\dot{A}+\dot{B})/2$ and $(\dot{C}+\dot{D})/2$, are also available. The symbol ∞ (infinity) means that the R_0 value is infinite. Isolation between ports ① and ② is sufficiently complete, as shown in Fig. 6, and the impedance of ports

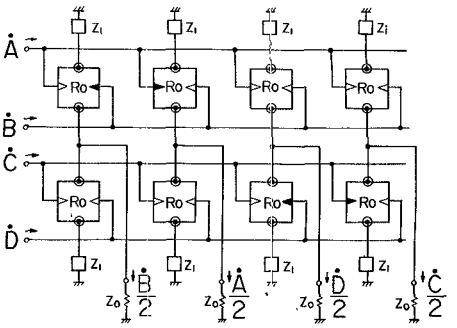

Fig. 11. 4×4 switch matrix using eight divider/combiner modules.

① and ② is very high compared with load impedance Z_0. Therefore, the above three outputs are independent of each other. This circuit is believed to be useful for vector combiners such as predistortors, phase shifters, and an adaptive linear combiner as the basic form of adaptive equalizer.

Fig. 11 shows a 4×4 switch matrix utilizing eight divider/combiner modules, where four circuits similar to that of Fig. 10 are cascaded. On-state GaAs FET's are represented by black triangles, and off-state GaAs FET's by white triangles. When the R_0 value and shunt impedance Z_i are infinite and Z_0 respectively, input signals $\dot{A}$, $\dot{B}$, $\dot{C}$, and $\dot{D}$ emerge in the order $\dot{B}/2$, $\dot{A}/2$, $\dot{D}/2$, and $\dot{C}/2$ in the operation mode shown in Fig. 11. For every input signal only one of the areas indicated by a triangle (two-gate GaAs FET) is in the on-state. Thus, a good impedance match is obtained at every input port. The size of these application circuits can be effectively minimized due to the very small magic T LUFET, and by using a thin-film microstrip (TFMS) line [8], [9] and its crossover structure.

Combining the divider/combiners and other control circuits such as phase shifters and attenuators will enhance the MMIC's functions. As a result, miniature ultra-wide-band divider/combiner modules, as well as the magic T LUFET, can be used as one of the fundamental function blocks for RF signal processing such as array antenna controls and multiport RF switching.

VI. Conclusion

An FET-sized ultra-wide-band MMIC magic T, called a magic T LUFET, is proposed and demonstrated through an analysis and experiments. Furthermore, characteristics of signal divider/combiners using a magic T and applications of a divider/combiner module to a multiport vector combiner and a 4×4 switch matrix have been discussed. Such miniaturized wide-band modules can be efficiently used for microwave and millimeter-wave MMIC's such as mixers and many types of RF signal processing circuits.

Acknowledgment

The authors would like to thank Dr. K. Habara, vice president of Advanced Telecommunications Research (ATR) Institute International, and Dr. Y. Furuhama, president of ATR Optical and Radio Communications Re-

search Laboratories, for their helpful discussions and valuable suggestions.

REFERENCES

[1] G. K. Lewis, I. J. Bahl, and E. L. Griffin, "GaAs MMICs for digital radio frequency memory (DRFM) sub-systems," in *IEEE Microwave and Millimeter-wave Monolithic Circuits Symp. Dig.*, 1987, pp. 53–56.

[2] R. K. Gupta, H. I. Gerson, P. B. Ross, and F. T. Assal, "Design and packaging approach for MMIC insertion in a broadband 4×4 microwave switch matrix," in *IEEE GaAs IC Symp. Dig.* Nov. 1988, pp. 261–264.

[3] G. S. Barta, K. E. Jones, G. C. Herrick, and E. W. Strid, "A 2 to 8 GHz leveling loop using a GaAs MMIC active splitter and attenuator," in *IEEE Microwave and Millimeter-wave Monolithic Circuits Symp. Dig.*, 1986, pp. 75–79.

[4] D. Levy, A. Noblet, and Y. W. Bender, "A 2–18 GHz monolithic phase shifter for electronic warfare phased array applications," in *IEEE GaAs IC Symp. Dig.* 1988, pp. 265–268.

[5] A. M. Pavio, R. H. Halladay, and S. D. Bingham, "Double balanced mixers using active and passive techniques," *IEEE Trans. Microwave Theory Tech.*, vol. 36, pp. 1948–1957, Dec. 1988.

[6] T. Tokumitsu, S. Hara, T. Tanaka, and M. Aikawa, "Active isolator, combiner, divider, and magic-T as miniaturized function blocks," in *IEEE GaAs IC Symp. Dig.* 1988, pp. 273–276.

[7] T. Tokumitsu, S. Hara, and M. Aikawa, "Very small, ultra-wideband MMIC magic-T and applications to combiners and dividers," in *IEEE MTT-S Int. Microwave Symp. Dig.* 1989, pp. 963–966.

[8] T. Hiraoka, T. Tokumitsu, T. Tanaka, and M. Aikawa, "Very small and wide band MMIC magic-T using microstrip line on a thin dielectric film," in *European Microwave Conf. Dig.* 1988, pp. 403–408.

[9] T. Hiraoka, T. Tokumitsu, and M. Aikawa, "Very small wide-band MMIC magic T's using microstrip lines on a thin dielectric film," *IEEE Trans. Microwave Theory Tech.*, vol. 37, pp. 1569–1575, Oct. 1989.

Tsuneo Tokumitsu (M'88) was born in Hiroshima, Japan, in 1952. He received the B.S. and M.S. degrees in electronics engineering from Hiroshima University, Hiroshima, in 1974 and 1976, respectively.

He joined the Yokosuka Electrical Communication Laboratories, Nippon Telegraph and Telephone Public Corporation, Yokosuka, in 1976, where he did research on microwave and millimeter-wave integrated circuits, MIC's, and MMIC's and worked on the development of onboard satellite equipment. In September 1986, he joined ATR Optical and Radio Communications Research Laboratories, Osaka, where he is currently engaged in research on highly integrated MMIC's for future digital mobile communications.

Mr. Tokumitsu is a member of the Institute of Electronics, Information and Communication Engineers of Japan.

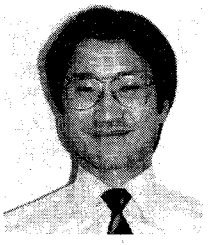

Shinji Hara (M'88) was born in Toyama, Japan, in 1960. He received the B.E. and M.E. degrees in electronics engineering from Waseda University, Tokyo, Japan in 1982 and 1984, respectively.

In 1984, he joined Tokyo Research Laboratories of the Sharp Corporation, Chiba, Japan. Since September 1986, he has been a researcher at ATR Optical and Radio Communications Research Laboratories, Osaka, Japan, on leave from the Sharp Corporation. At ATR, he has been engaged in research on circuit design technologies to realize highly integrated MMIC's.

Mr. Hara is a member of the Japan Society of Applied Physics and the Institute of Electronics, Information and Communication Engineers of Japan.

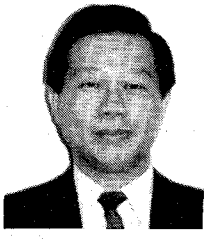

Masayoshi Aikawa (M'78) was born in Saga, Japan, on October 16, 1946. He received the B.S., M.S., and Dr. Eng. degrees in electronics engineering from Kyushu University, Fukuoka, Japan, in 1969, 1971, and 1985, respectively.

In 1971, he joined the Musashino Electrical Communication Laboratories, Nippon Telegraph and Telephone Public Corporation. Tokyo, Japan, where he did research and development work on microwave and millimeter-wave integrated circuits, MIC's, MMIC's, and equipment for 20 GHz digital radio trunk transmission systems and 26 GHz subscriber radio systems. In 1986, he joined ATR Optical and Radio Communications Research Laboratories, Osaka, Japan, where he was engaged in research on basic techniques for future digital mobile communications. He is now with the NTT Radio Communication Systems Laboratories, Yokosuka, where he has been engaged in research and development work on monolithic microwave and millimeter-wave integrated circuits and their applications.

Dr. Aikawa is a member of the Institute of Electronics, Information and Communication Engineers of Japan.